

Strategies for an accurate determination of the X(3872) energy  
from QCD lattice simulationsE. J. GARZON<sup>a)</sup>, R. MOLINA<sup>b)</sup>, A. HOSAKA<sup>c)</sup> AND E. OSET<sup>a)</sup>*a) Departamento de Física Teórica and IFIC, Centro Mixto Universidad de Valencia-CSIC, Institutos de Investigación de Paterna, Aptdo. 22085, 46071 Valencia, Spain.**b) The George Washington University, Corcoran Hall 725 21st Street NW Room 105 Washington, DC 20052, USA.**c) Research Center for Nuclear Physics (RCNP), Osaka University, Ibaraki, Osaka 567-0047, Japan*

We develop a method to determine accurately the binding energy of the X(3872) from lattice data for the  $D\bar{D}^*$  interaction. We show that, because of the small difference between the neutral and charged components of the X(3872), it is necessary to differentiate them in the energy levels of the lattice spectrum if one wishes to have a precise determination of the the binding energy of the X(3872). The analysis of the data requires the use of coupled channels. Depending on the number of levels available and the size of the box we determine the precision needed in the lattice energies to finally obtain a desired accuracy in the binding energy.

PRESENTED AT

The 7th International Workshop on Charm Physics  
(CHARM 2015)  
Detroit, MI, 18-22 May, 2015

# 1 Introduction

The purpose of the present paper is to find a strategy to determine accurately the binding energy of the X(3872) in lattice QCD simulations. A precise determination, with an energy about 0.2 MeV below the  $D^0\bar{D}^{*0}$  threshold, requires to differentiate between the  $u$  and  $d$  quark masses in order to account for the 7 MeV difference between the neutral and charged components of the wave function [1]. The small binding of the state with respect to the  $D^0\bar{D}^{*0}$  threshold, much smaller than the difference of masses between the  $D^0\bar{D}^{*0}$  and  $D^+D^{*-}$  components, makes this consideration imperative in order to get a precise value of the binding energy and unambiguously determine the bound state character of the X(3872). In fact, when this is done, energy levels can be associated to either  $D^0\bar{D}^{*0}$  or  $D^+D^{*-}$ .

## 2 The X(3872) in the continuum limit

In this section we discuss briefly the dynamical generation of the X(3872) in the continuum limit. All the details are in Refs. [1, 2]. The pseudoscalar - vector interaction can be studied through the hidden gauge Lagrangian [3], which contains interaction between vectors and with pseudoscalar mesons. The model is based on vector-meson exchange, see Fig. 1. In fact, for s-wave, when the momenta  $q^2$  exchanged in the

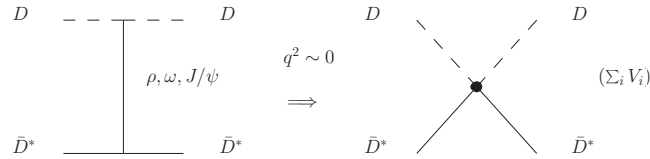


Figure 1: Point-like pseudoscalar - vector interaction.

propagator of the vector meson exchanged can be neglected against  $-M_V^2$ , leads to a point-like interaction, and is equivalent to using the Lagrangian,

$$\mathcal{L}_{PPVV} = -\frac{1}{4f^2} \text{Tr} (J_\mu \mathcal{J}^\mu). \quad (1)$$

with  $J_\mu = (\partial_\mu P)P - P\partial_\mu P$  and  $\mathcal{J}_\mu = (\partial_\mu \mathcal{V}_\nu)\mathcal{V}^\nu - \mathcal{V}_\nu\partial_\mu \mathcal{V}^\nu$ , see [1, 4]. In Ref. [1], the currents are separated for heavy and light vector-meson-exchange, introducing the breaking parameters,  $\gamma = \left(\frac{m_{8^*}}{m_{3^*}}\right)^2 = \frac{m_L^2}{m_H^2}$ ,  $\psi = \left(\frac{m_{8^*}}{m_{1^*}}\right)^2 = \frac{m_L^2}{m_{J/\psi}^2}$ , with  $m_{8^*} = m_L = 800$  MeV,  $m_{3^*} = m_H = 2050$  MeV and  $m_{1^*} = m_{J/\psi} = 3097$  MeV. This gives,  $\gamma = 0.14$  and  $\psi = 0.07$ . Because of the smallness of the breaking parameters, the light and heavy

sector are almost disconnected, and the transition potential between those is very small. Also, for light mesons,  $f = f_\pi = 93$  MeV, and for heavy ones,  $f = f_D = 165$  MeV, is used. Thus, the amplitude of the process  $V_1(k)P_1(p) \rightarrow V_2(k')P_2(p')$ , is given by

$$V_{ij}(s, t, u) = \frac{\xi_{ij}}{4f_i f_j}(s - u) \vec{\epsilon} \cdot \vec{\epsilon}' \quad (2)$$

with  $s - u = (k + k')(p + p')$ , which must be projected in s-wave [1, 4], and  $i, j$  refer to the particle channels. Working in the charge basis, we have the channels  $\frac{1}{\sqrt{2}}(\bar{K}^{*-} K^+ - c.c.)$ ,  $\frac{1}{\sqrt{2}}(\bar{K}^{*0} K^0 - c.c.)$ ,  $\frac{1}{\sqrt{2}}(D^{*+} D^- - c.c.)$ ,  $\frac{1}{\sqrt{2}}(D^{*0} \bar{D}^0 - c.c.)$  and  $\frac{1}{\sqrt{2}}(D_s^{*+} D_s^- - c.c.)$ , and the matrix  $\xi$  can be written in this basis as

$$\xi = \begin{pmatrix} -3 & -3 & 0 & -\gamma & \gamma \\ -3 & -3 & -\gamma & 0 & \gamma \\ 0 & -\gamma & -(1 + \psi) & -1 & -1 \\ -\gamma & 0 & -1 & -(1 + \psi) & -1 \\ \gamma & \gamma & -1 & -1 & -(1 + \psi) \end{pmatrix}. \quad (3)$$

Eq. (2) is the input of the Bethe Salpether equation,

$$T = (I - VG)^{-1} V \vec{\epsilon} \cdot \vec{\epsilon}'. \quad (4)$$

Here  $G$  a diagonal matrix of the two-meson loop function for each channel. Usually it is evaluated with dimensional regularization and depends on the parameter  $\alpha$  [1] or one can also evaluate the  $G$  function with a cutoff. The calculation in Ref. [1] is redone to get a binding energy more realistic at 0.2 MeV with respect to the channel  $D^{*0} \bar{D}^0 - c.c.$  [2], where the masses of the mesons are taken from the PDG [5]. The free parameter,  $\alpha$ , is fixed for the light channels,  $\alpha_L = -0.8$  [1, 4], but the pole position of the X(3872) is not sensitive to that, since its mass is far away from these thresholds. For the heavy channels, the value  $\alpha_H = -1.265$  is needed for such binding energy ( $\mu$  is taken equal to 1500 MeV in all channels). In Table 1, a summary of the pole position and couplings of the resonance to each channel is given. The Weinberg compositeness condition [6] can be generalized for dynamically generated resonances from several channels [1] and gives the probability of finding the  $i$  channel in the wave function, which are 0.86 for  $D^{*0} \bar{D}^0 - c.c.$ , 0.124 for  $D^{*+} D^- - c.c.$  and 0.016 for  $D_s^{*+} D_s^- - c.c.$  However, this is different from the wave function at the origin  $(2\pi)^{3/2} \psi(0)_i = g_i G_i$ , which usually enters the evaluation of observables and are nearly equal [1].

### 3 Formalism in finite volume

We follow the formalism used Ref. [7] where the infinite volume amplitude  $T$  is replaced by the amplitude  $\tilde{T}$  in a finite box of size  $L$  and  $G(P^0)$  is replaced by the finite

| $\sqrt{s_0} = (3871.6 - i0.001) \text{ MeV}$ |                       |
|--|-----------------------|
| Channel                                      | $ g_i  \text{ [MeV]}$ |
| $\frac{1}{\sqrt{2}}(K^{*-}K^+ - c.c)$        | 53                    |
| $\frac{1}{\sqrt{2}}(\bar{K}^{*0}K^0 - c.c)$  | 49                    |
| $\frac{1}{\sqrt{2}}(D^{*+}D^- - c.c)$        | 3638                  |
| $\frac{1}{\sqrt{2}}(D^{*0}\bar{D}^0 - c.c)$  | 3663                  |
| $\frac{1}{\sqrt{2}}(D_s^{*+}D_s^- - c.c)$    | 3395                  |

Table 1: Couplings of the pole at  $\sqrt{s_0}$  MeV to the channel  $i$ .

volume loop function denoted with  $\tilde{G}$ , given by the discrete sum over eigenstates of the box

$$\tilde{G}(P^0) = \frac{1}{L^3} \sum_{\vec{q}_i} I(P^0, \vec{q}_i) \quad (5)$$

with

$$I(P^0, \vec{q}_i) = \frac{\omega_1(\vec{q}_i) + \omega_2(\vec{q}_i)}{2\omega_1(\vec{q}_i)\omega_2(\vec{q}_i)} \frac{1}{(P^0)^2 - (\omega_1(\vec{q}_i) + \omega_2(\vec{q}_i))^2} \quad (6)$$

where  $\omega_i = \sqrt{m_i^2 + |\vec{q}_i|^2}$  is the energy and the momentum  $\vec{q}$  is quantized as  $\vec{q}_i = \frac{2\pi}{L}\vec{n}_i$ , corresponding to the periodic boundary conditions. Here the vector  $\vec{n}$ , denotes the three dimension vector of all integers ( $\mathbb{Z}^3$ ). This form produces a degeneracy for the set of three integer which has the same modulus. The sum over the momenta is done until a  $q_{max}$ , so the three dimension sum over  $\vec{n}_i$  in Eq. (5) becomes a one dimension sum over  $m_i$  to an  $n_{max}$  in a symmetric box,  $n_{max} = \frac{q_{max}L}{2\pi}$ . The equivalent formalism in finite volume should also be made independent of  $q_{max}$  and related to  $\alpha$ . This is done in Ref. [8] with the result

$$\tilde{G} = G^{DR} + \lim_{q_{max} \rightarrow \infty} \left( \frac{1}{L^3} \sum_{q < q_{max}} I(P^0, \vec{q}) - \int_{q < q_{max}} \frac{d^3q}{(2\pi^3)} I(P^0, \vec{q}) \right) \equiv G^{DR} + \lim_{q_{max} \rightarrow \infty} \delta G. \quad (7)$$

In Fig. 2 we show that  $\delta G$  converges as  $q_{max} \rightarrow \infty$ . In practice, one can take an average for different values between  $q_{max} = 1500-2500$  MeV and one sees that it reproduces fairly well the limit of  $q_{max} \rightarrow \infty$ . The Bethe-Salpeter equation in finite volume, can be written as,

$$\tilde{T}^{-1} = V^{-1} - \tilde{G} \quad (8)$$

The energy levels in the box in the presence of interaction  $V$  correspond to the condition

$$\det(I - V\tilde{G}) = 0. \quad (9)$$

In a single channel, Eq. (9) leads to poles in the  $\tilde{T}$  amplitude when  $V^{-1} = \tilde{G}$ . Furthermore, for one channel, we can write the amplitude in infinite volume  $T$  for

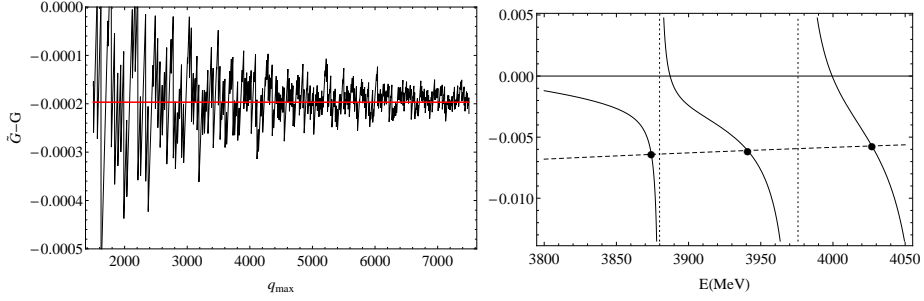


Figure 2: Left: Representation of  $\delta G = \tilde{G} - G$  for  $D^+D^{*-}$  in function of  $q_{max}$  for  $\sqrt{s} = 3850$  MeV. The thick line represents the average of  $\delta G$  for different values of  $q_{max}$  between 1500 and 2500 MeV. Right:  $\tilde{G}$ (solid) and  $V^{-1}$ (dashed) energy dependence of  $D^+D^{*-}$  for  $Lm_\pi = 2.0$ . Black dots correspond to energies ( $E \equiv P^0$ ) where  $V^{-1} = \tilde{G}$ . Vertical dotted lines are the free energies in the box for  $DD^*$ .

the energy levels ( $E_i$ ) as

$$T = (\tilde{G}(E_i) - G(E_i))^{-1}. \quad (10)$$

## 4 Two channel case

In the work [1] (see also [1, 2]), a pole at  $\sqrt{s} = 3871.6$  MeV is obtained using a subtraction constant of  $\alpha_H = -1.265$ , with a binding energy of 0.2 MeV with respect to the neutral channel. When we address the inverse problem in the next section, for the sake of simplicity, we take only two channels,  $D^+D^{*-}$  and  $D^0\overline{D}^{*0}$ , reevaluating the coupled channel calculation explained in section II (see Table 1). Then, a new value  $\alpha_H = -1.153$  is needed in order to get the same position of the pole. The novelty of this study is the inclusion of two channel in the finite box, where the energies are found using the condition of Eq. (9). As one can see in Fig. 3 we have two curves for each level, when for a single channel we had only a trajectory of the energy for each level. This feature is understood looking into Fig. 3, where the free energies for the channels  $D^+D^{*-}$  and  $D^0\overline{D}^{*0}$  are the dotted lines. Since the determinant of Eq. 9 has a zero between two asymptotes, the number of bound states in the box is doubled.

## 5 The inverse problem

Once we have determined the dependence of poles of  $\tilde{T}$  with  $L$  using the potential for the  $DD^*$ , we want now to study the inverse problem. The idea is that QCD lattice data can be used to determine bound states of the  $D\overline{D}^*$  system. For this purpose we assume that the lattice data are some discrete points on the energy trajectories

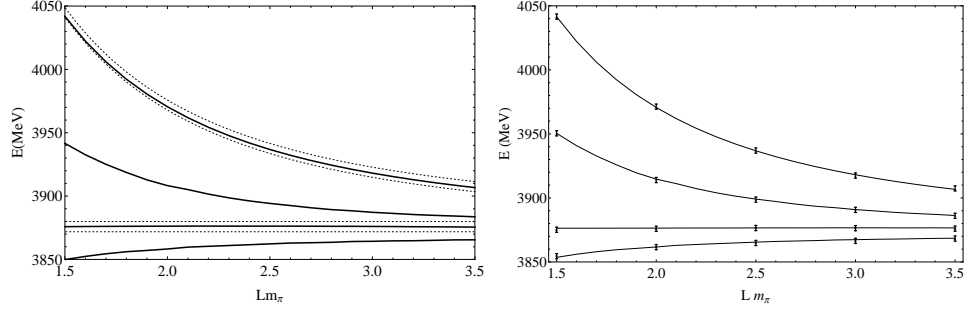


Figure 3: Left:  $L$  dependence of the energies of the poles for the two first levels of  $D^+D^{*-}$  and  $D^0\overline{D}^{*0}$ . Dotted lines correspond to the free energies. Right: Fit to the data. Dots with error bar are the synthetic data generated as explained in the text. Solid lines show the results obtained using the potential fitted to the synthetic data.

obtained by us. Thus, we generate a set of data for some  $L$  for a value of the subtraction constant  $\alpha = -1.153$ . In this case we generate 5 points in a range of  $Lm_\pi = [1.5, 3.5]$  and take 4 levels, this corresponds to  $n=0$  and 1 in the momentum for both channels  $D^+D^{*-}$  and  $D^0\overline{D}^{*0}$ . In addition, we simulate uncertainties in the obtained data, moving randomly by 1 MeV the centroid of the energies, then we assign an error of 2 MeV to these data. In Fig. 3 we show the simulated set of data. The second step is to choose the potential. We have chosen a potential with linear dependence in  $\sqrt{s}$ . This is given by

$$V_i = a_i + b_i \left( \sqrt{s} - \sqrt{s^{th}} \right) \quad (11)$$

where  $\sqrt{s^{th}} = m_{D^0} + m_{\overline{D}^{*0}}$  is the energy of the first threshold, and  $i=1, 2$  and 3 are the indices for each channel ( $i=1$  for  $D^+D^{*-}$ ,  $i=2$  for  $D^0\overline{D}^{*0}$  and  $i=3$  for the nondiagonal potential). Therefore, there are six parameters to determine in the potential. With all these ingredients, we do the fit, evaluating those values of the parameters in Eq. (11) that minimize the  $\chi^2$  function. The error band is obtained in the standard method [7] varying randomly the parameters of the potential in a moderate range (10% change) and choosing the set of parameters that satisfy the condition  $\chi^2 \leq \chi_{min}^2 + 1$ . With these sets of parameters we determine the binding energy of the system with its dispersion from the pole of  $T = (V^{-1} - G^{DR})^{-1}$ . In both  $\tilde{T}$  and  $T$  we need a value of  $\alpha$  to determinate  $\tilde{G}$  or  $G^{DR}$ . The interesting thing that we observe is that the results for the binding energy are essentially independent of the choice of  $\alpha$ . Changes in  $\alpha$  revert on changes of  $V$  that compensate for it. We made choices of  $\alpha_H$  between -1.2 and -2.2.

| Data |   |            |            | Parameters |         |         |        |        |        | Results  |         |           |          |
|------|---|------------|------------|------------|---------|---------|--------|--------|--------|----------|---------|-----------|----------|
| B    | P | $\Delta E$ | $\Delta C$ | $a_1$      | $a_2$   | $a_3$   | $b_1$  | $b_2$  | $b_3$  | $\chi^2$ | Pole    | Mean Pole | $\sigma$ |
| 4    | 5 | 2          | 1          | -140.18    | -112.08 | -132.81 | -0.310 | 0.074  | 0.012  | 2.32     | 3871.51 | 3871.49   | 0.07     |
| 4    | 5 | 5          | 2          | -140.18    | -112.08 | -132.81 | -0.310 | 0.074  | 0.012  | 0.79     | 3871.51 | 3871.25   | 0.38     |
| 4    | 3 | 2          | 1          | -133.01    | -131.92 | -124.60 | -0.242 | 0.048  | -0.075 | 1.02     | 3871.44 | 3871.49   | 0.18     |
| 4    | 3 | 5          | 2          | -120.09    | -98.19  | -150.94 | -0.377 | -0.075 | 0.102  | 0.28     | 3871.41 | 3871.15   | 0.49     |
| 2    | 5 | 2          | 1          | -176.08    | -154.11 | -89.26  | 9.92   | 7.01   | -8.72  | 0.259    | 3871.70 | 3871.47   | 0.30     |
| 2    | 5 | 5          | 2          | -158.49    | -152.15 | -103.23 | 4.56   | 6.58   | -6.74  | 0.982    | 3871.34 | 3871.30   | 0.43     |
| 2    | 3 | 2          | 1          | -132.74    | -176.62 | -105.53 | 3.23   | 0.84   | -3.36  | 0.074    | 3870.51 | 3870.48   | 0.61     |
| 2    | 3 | 5          | 2          | -226.57    | -194.51 | -32.74  | 31.81  | 13.28  | -18.89 | 0.942    | 3869.49 | 3870.37   | 1.06     |

Table 2: All possible set up changing number of branches ( $B$ ), number of points ( $P$ ), energy error bar ( $\Delta E$ ) and centroid of the energies ( $\Delta C$ ) and their set of parameters fitted. The columns denoted as Results are the  $\chi^2$  obtained in the fit, the pole is determined with the parameters, and the mean pole and the dispersion are calculated as explained in the text. The results are for  $\alpha = -1.25$ . As noted in the text, the use of different values of  $\alpha$  change the potential but not the binding energy. Note that we quote values of total  $\chi^2$  not the reduced one, which is always much smaller than 1.

## 6 Results

The results of the fits are shown in Table 2, where the first four columns determine the chosen set up of the synthetic data. The next columns are the fitted parameters, value of  $\chi^2$  and pole position. The energy values in the “Pole” column correspond to the pole positions of the  $T$  matrix using the  $G^{DR}$  loop function evaluated with dimensional regularization together with the parametrized potential of Eq. (11). To test the stability of the pole with the parameters, we vary randomly the parameters by 10%. If the new  $\chi^2$  calculated with those parameters is less than the  $\chi^2$  obtained in the fit plus one, we determine the pole position, otherwise it will be discarded. We iterate several times until we get 20 or 30 values of the pole positions. Then, we calculate the mean value of those pole positions and their dispersion  $\sigma$ . The results are in the line with one should expect: fewer branches, fewer points or bigger errors which reverts into a higher dispersion in the binding energy. Since it is difficult for Lattice simulations to calculate higher levels, we have done also the test for the first level of energies for both channels, and in all cases the dispersion of the pole is higher than in the case where two levels are taken into account. Since the experimental errors in the binding of the  $X(3872)$  are of the order of 0.20 MeV, the exercise done is telling the level of precision demanded for the Lattice data if the experimental precision is to be matched.

## 7 Conclusions

We have studied the  $X(3872)$  state using coupled channels  $D^+D^{*-}$  and  $D^0\overline{D}^{*0}$  in a finite box. This is done for a small binding energy. We have observed that in order to get a good precision in the binding energy, one does not need to extract the lattice

data with very small errors. Indeed, even with errors in the data points of 5 MeV, one can obtain the binding energy with 1 MeV (or even smaller value) precision. From a practical point of view, knowing that it is difficult to get four levels in actual Lattice calculations, it is rewarding to see that with only two levels one can get quite an accurate value for the binding, provided the levels are evaluated at several values of  $L$  with enough precision. We hope that this work gives a reference in the study of Lattice QCD for best strategies in order to obtain optimum values of the binding of the  $X(3872)$  state.

## References

- [1] D. Gamermann and E. Oset, Phys. Rev. D **80**, 014003 (2009). D. Gamermann, J. Nieves, E. Oset and E. Ruiz Arriola, Phys. Rev. D **81**, 014029 (2010). D. Gamermann and E. Oset, Eur. Phys. J. A **33**, 119 (2007)
- [2] F. Aceti, R. Molina and E. Oset, Phys. Rev. D **86**, 113007 (2012)
- [3] M. Bando, T. Kugo, S. Uehara, K. Yamawaki and T. Yanagida, Phys. Rev. Lett. **54**, 1215 (1985). M. Bando, T. Kugo and K. Yamawaki, Phys. Rept. **164**, 217 (1988). M. Harada and K. Yamawaki, Phys. Rept. **381**, 1 (2003). U. G. Meissner, Phys. Rept. **161**, 213 (1988).
- [4] L. Roca, E. Oset and J. Singh, Phys. Rev. D **72**, 014002 (2005)
- [5] J. Beringer *et al.* [Particle Data Group], Phys. Rev. D **86**, 010001 (2012)
- [6] S. Weinberg, Phys. Rev. **137**, B672 (1965).
- [7] M. Doring, U. -G. Meissner, E. Oset and A. Rusetsky, Eur. Phys. J. A **47**, 139 (2011).
- [8] A. Martinez Torres, L. R. Dai, C. Koren, D. Jido and E. Oset, Phys. Rev. D **85**, 014027 (2012)